

# A Bragg Detector Built for AMS Purposes

G.M. Santos<sup>1,\*</sup>, J.C. Acquadro<sup>2</sup>, R.M. Anjos<sup>1,\*</sup>, N. Added<sup>2,\*</sup>, R. Liguori Neto<sup>2,\*</sup>,  
P.R.S. Gomes<sup>1,\*†</sup>, M.A. Rizzuto, N.H. Medina<sup>2,\*</sup>, N. Carlin<sup>1,\*</sup>

<sup>1</sup> Instituto de Física,

Universidade Federal Fluminense,

Av. Litoranea s/n, Gragoatá, Niterói, R.J., 24210-340, Brazil

<sup>2</sup>Instituto de Física, Universidade de São Paulo,

C.P. 20516, S. Paulo, 01498-970, Brazil

Recebido 22 de Abril, 1998

A Bragg detector has been designed and built. In this paper, results of tests, performed with different scattered beams, are reported. The energy resolution of 1.7% and charge resolutions of 1.3% show that it is suitable to be used in the Brazilian AMS program.

Um detetor de Bragg foi projetado e construído. Neste artigo são mostrados os resultados de seus testes, realizados com diferentes feixes incidentes. Resoluções em energia de 1.7% e em número atômico de 1.3% mostram que o detetor é apropriado para ser usado no Programa Brasileiro de AMS.

## I Introduction

The Accelerator Mass Spectrometry (AMS) technique is, at the present, the most powerful method for mass spectrometry[1]. It is particularly attractive since it allows the determination of concentrations with a sensitivity down to 1 atom of isotope in  $10^{15}$  atoms, using few milligrams samples. The determination of these extremely low concentrations of rare isotopes is accomplished using a Tandem accelerator as a magnetic and electrostatic analyzer and detection good enough to identify unambiguously each ion.

In the last few years, efforts have been devoted to the implementation of this technique in Brazil. Different institutions are involved with it. The accelerator used is the Pelletron 8UD Tandem at USP. The initial major emphases are on projects based on the determination of  $^{36}\text{Cl}$ ,  $^{26}\text{Al}$ ,  $^{14}\text{C}$  and  $^{10}\text{Be}$  concentrations, with main applications on geological dating archaeology, climatology, environmental and biological studies.

One may say that one of the main technical problems when dealing with the ultra high sensitive AMS technique is the presence of isobaric contamination on natural samples, like  $^{10}\text{B}$  in  $^{10}\text{Be}$ ,  $^{26}\text{Mg}$  in  $^{26}\text{Al}$  and  $^{36}\text{S}$  in  $^{36}\text{Cl}$ . In all these examples, the chemical sepa-

ration of the contaminants, in the levels required for AMS purposes, is very difficult. Therefore, one needs a detection system that is able to separate elements that differ by one unit of charge in the mass energy region of interest. Complex systems, as multi-anode ionization chambers, magnetic spectrometers, electrostatic detectors, gas-filled magnets and velocity filters may also be used in the application of the AMS technique.

Preliminary tests of the detection of unstable beams were performed in the laboratory with a position sensitive ionization chamber, coupled with a silicon barrier position sensitive detector [2,3]. The specific energy loss of the incident particle in the gas is proportional to its  $Z^2$  and it is dependent on its energy. The gas detector measures the energy loss  $\Delta E$  and the solid state detector measures its residual energy. The electric field between anode and cathode is perpendicular to the particle incident direction. The analysis of the energy and the biparametric  $E \times \Delta E$  spectra for the  $^{26}\text{Al}$  and  $^{36}\text{Cl}$  measurements have shown that, although the peak positions of the isobars could be separated, the background tails of  $^{36}\text{S}$  and  $^{26}\text{Mg}$  on the  $^{36}\text{Cl}$  and  $^{26}\text{Al}$  spectra were too high to be used for AMS purposes. The energy loss resolution of this detector is of the order

\*Fellow of the Conselho Nacional de Desenvolvimento Científico e Tecnológico - CNPq

†Autor para contato: Paulo R. S. Gomes. Fone e fax: (021) 620 6735, E-mail: paulogom@if.uff.br

of 4%. Therefore, we decided to change the detection system.

A new detector has been designed and built at UFF and USP: a Bragg detector (BD)[4,5]. This kind of detector has been used before[6,7] for AMS purposes. It is expected to have good energy and charge resolution over a wide range of atomic number and energy. In this paper we report on the performance of this detector. Section 2 describes the general characteristics of a BD. In section 3 the design of our BD is described. Results of tests are shown in section 4. In section 5 a summary is presented.

## II Bragg detector general characteristics

A Bragg detector has an applied electric field parallel to the incident particle direction, and enough gas pressure to stop it[4,5]. This last property allows the determination of the range of particle in the detection medium, and its total energy. The nuclear charge of the particle can be obtained by determining the portion of the energy that the particle has lost over a given path length and the spatial distribution of electrons produced along the path of the particles in the gas (the so-called Bragg curve). The range of the particle is proportional to its  $A/Z^2$  ratio. The time dependence of the ionization current collected at the anode is related with the Bragg curve and, therefore, the range of the particles is determined by the time length of the signal. Identical particles at different energies differ in their range but have roughly the same specific ionization in their Bragg maxima. Projectiles with different nuclear charges have different specific ionization at their Bragg maxima. For isobars, the ratio of their range is equal to their  $Z^2$  ratio. Therefore, the nuclear charge of the particle is obtained by integration of the specific ionization around the Bragg peak, while the total energy is obtained, as usual, from the total ionization current.

The discrimination between the ionization near the Bragg maximum (charge identification signal) and the total ionization (total energy signal) is obtained by the use of two main amplifiers, with different shaping times, after the split of the output signal from the pre-amplifier. For the total ionization, the shaping time is longer than the total electron collection time ( $> 6\mu s$ ), while the other one operates with shaping time of the order of the collection time of the electrons from the Bragg maximum (from 0.1 to 0.5  $\mu s$ ).

## III Detector Design

Figure 1 shows a schematic layout of our Bragg detector. It has a cylindrical geometry and contains 12 equipotential guard rings separated by ceramic rings. The detector assembly is a spare part of the S. Paulo's 8UD NEC Pelletron accelerator tube, made of stainless steel. Figures 2a and 2b are pictures of the detector. The diameter and length of the active detector volume are 5.3 cm 15.5 cm, respectively. The entrance window, made of aluminized mylar foils, works as cathode. The inner diameter of the window is 2.7 cm and its thickness is 1.7  $\mu m$  (230  $\mu g/cm^2$ ).

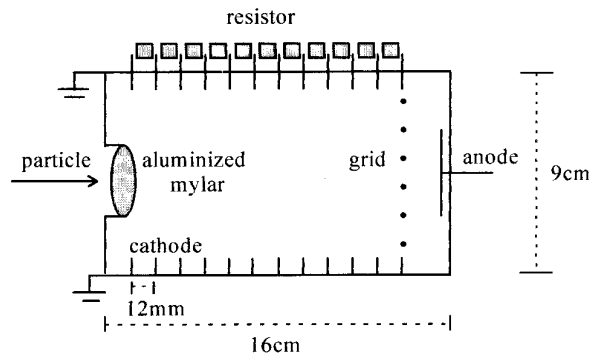


Figure 1. Schematic layout of the Bragg detector.

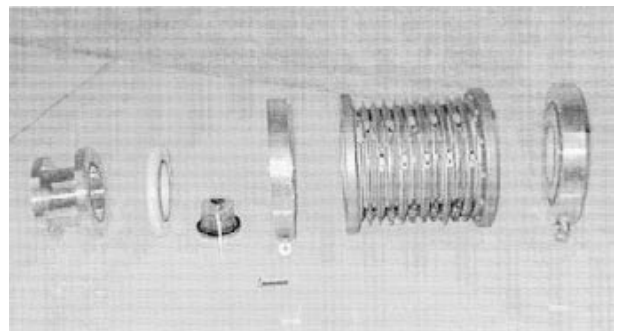


Figure 2a. Picture of the Bragg detector parts.

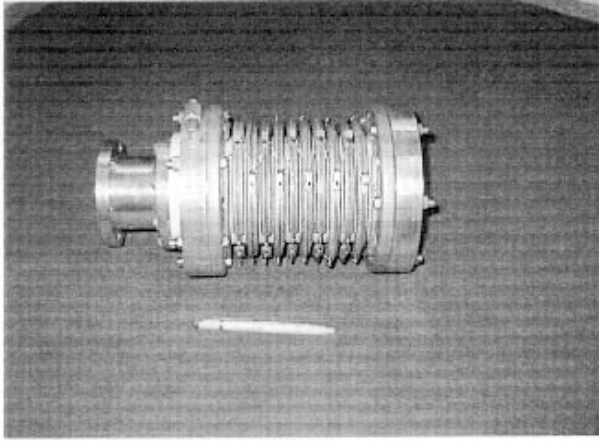


Figure 2b. Picture of the Bragg detector.

The electrons produced by the particle in gas ionization process drift to the anode and start inducing a signal when they cross the Frisch grid. The grid consists of parallel  $20\ \mu\text{m}$  tungsten wires coated with flash of Au, separated by 1 mm. A constant drift velocity is

obtained applying a voltage to the rings, which produce a homogeneous electric field along the drift direction. The rings are 12 mm apart from each other. The Frisch grid efficiency is 98.3% and it is located at 10 mm from the anode and 155 mm from the cathode (active depth). A chain of 11 resistors of  $100\ \text{K}\Omega$  is used as a voltage divider between the Frisch grid and the cathode. The anode consists of a Cu round plate with 65 mm diameter. In order to avoid charge collection on the Frisch grid, the electric field on the region between the grid and the anode must be higher than in the region between the cathode and the grid.

The gas used is the usual P 10 (90% Ar, 10%  $\text{CH}_4$ ). For the beam energies of interest,  $8 \leq Z \leq 17$ ,  $45\ \text{MeV} \leq E_{\text{Lab}} \leq 72\ \text{MeV}$ , calculations performed by the TRIM[8] code have shown that the gas pressure required to stop the detected particles are within the range from 120 to 200 Torr.

Table 1 summarizes the design parameters of our Bragg detector.

Table 1. Design parameters of the Bragg detector

cathode to grid distance	155 mm
grid to anode distance	10 mm
grid wire diameter	$20\ \mu\text{m}$
grid wire spacing	1 mm
cathode window diameter	27 mm
cathode window thickness	$1.7\ \mu\text{m}$ ( $230\ \mu\text{m}/\text{cm}^2$ )
grid efficiency	98.3%
geometrical transmission	97.5%
gas	P 10 (10% $\text{CH}_4$ , 90% Ar)

## IV Detector Performance

The first tests of the BD were performed with beams of  $^{28}\text{Si}$ ,  $^{35,37}\text{Cl}$  and  $^{32}\text{S}$  ( $Z = 14, 16, 17$ ). The voltage terminal was kept fixed, and therefore, due to their different charge states, the beams had different energies on a  $^{197}\text{Au}$  target. The beam energies used were in the range from 45 MeV to 72 MeV.

During the first tests, the BD was fixed at the extremity of a large multipurpose scattering chamber, at  $15^\circ$  with the beam direction. The gas pressure was set at 165 Torr. During the tests we have noticed that it

had changed within 10% of this value, causing some deterioration in the detector performance. A new control of the gas pressure is being built. Further tests, with  $^{35}\text{Cl}$ ,  $^{37}\text{Cl}$  and  $^{36}\text{S}$  beams, were performed with the detector placed at zero degree with the beam direction, as shown in figure 3. A much better gas pressure stability was achieved using a higher gas flux.

Tests have been performed varying the detector, grid and anode voltages. The optimum conditions were achieved for a detector bias of 1000 V; Frisch grid and anode voltages at 100 V and 200 V, respectively. These values lead to a cathode-Frisch grid field of  $73.3\ \text{V}/\text{cm}$

and a grid - anode field of 100 V/cm. For the gas pressure of 165 Torr, this corresponds to reduced fields of 0.61 V/cm Torr and 0.44 V/cm Torr, respectively. The ratio grid-anode field / cathode-grid field, for these conditions, is 1.37.

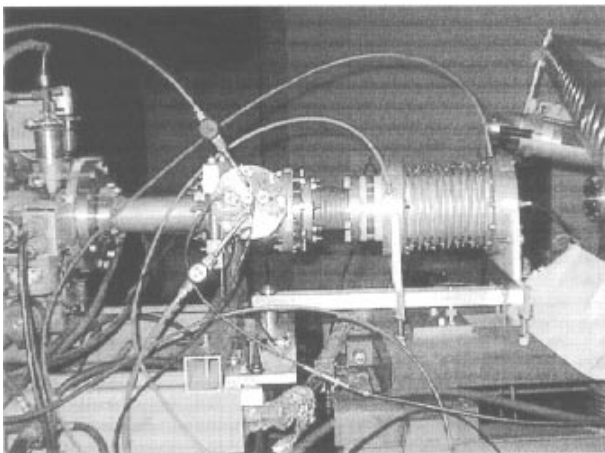


Figure 3. The detector placed at zero degree with the Pelletron beam direction.

Best values for amplifier shaping time were also checked. For the total energy signal, the values of 3 and 6  $\mu$ s leads to similar resolutions, and the longer one was then used. For the charge signals, a short shaping time is required in order to the signals be independent of the particle energies. That was achieved for the shortest

shaping time of the Mechtronics 510 amplifier, 0.2  $\mu$ s.

Figure 4a shows the biparametric spectra of the Bragg Peak versus Total Energy for the  $^{28}\text{Si}$ ,  $^{37}\text{Cl}$  and  $^{32}\text{S}$  scattered beams, and the detector placed at  $15^\circ$ . Actually this figure shows the superposition of 3 different spectra, one for each beam. The beam energies are in the range from 64 MeV to 68 MeV. One can notice that the Z signals are independent of the energy for each beam and that unique Z separation is obtained, with very good separation of the elements. The projection of the spectra on the Bragg peak axis is shown in figure 4b.

Figure 5c shows the superposition of biparametric spectra of  $^{35}\text{Cl}$ ,  $^{37}\text{Cl}$  and  $^{36}\text{S}$  beams, taken with the detector at zero degree and energies of 64.0 MeV, 60.5 MeV and 62.4 MeV, respectively. Figures 5a and 5b are the projection energy and energy loss spectra, respectively. One can notice that the  $^{36}\text{S}$  counts are well separated from the  $^{35,37}\text{Cl}$ , as it should be from the  $^{36}\text{Cl}$ .

The detector energy resolution  $\Delta E(\text{FWHM}) / E$  achieved was 1.7% for these beams. The charge resolution resolution  $\Delta Z(\text{FWHM}) / Z$  was derived to be 1.3%. The separation between the positions of the peaks of two adjacent elements(  $(C_{17} - C_{16}) / C_{17}$ ) is 8.6%.

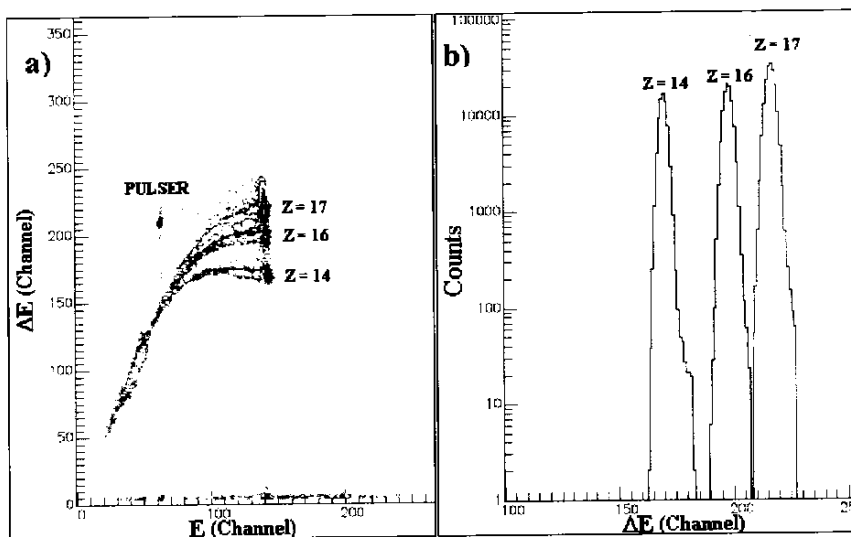


Figure 4a. Biparametric spectra of the Bragg Peak versus Total Energy for the  $^{28}\text{Si}$ ,  $^{37}\text{Cl}$  and  $^{32}\text{S}$  scattered beams, and the detector placed at  $15^\circ$ . The beam energies are in the range 64 - 68 MeV. An auxiliary pulser response is present in the spectra. Figure 4b. The projection of the spectra of figure 4a on the Bragg peak axis, with energy calibration of 0.30 MeV/channel.

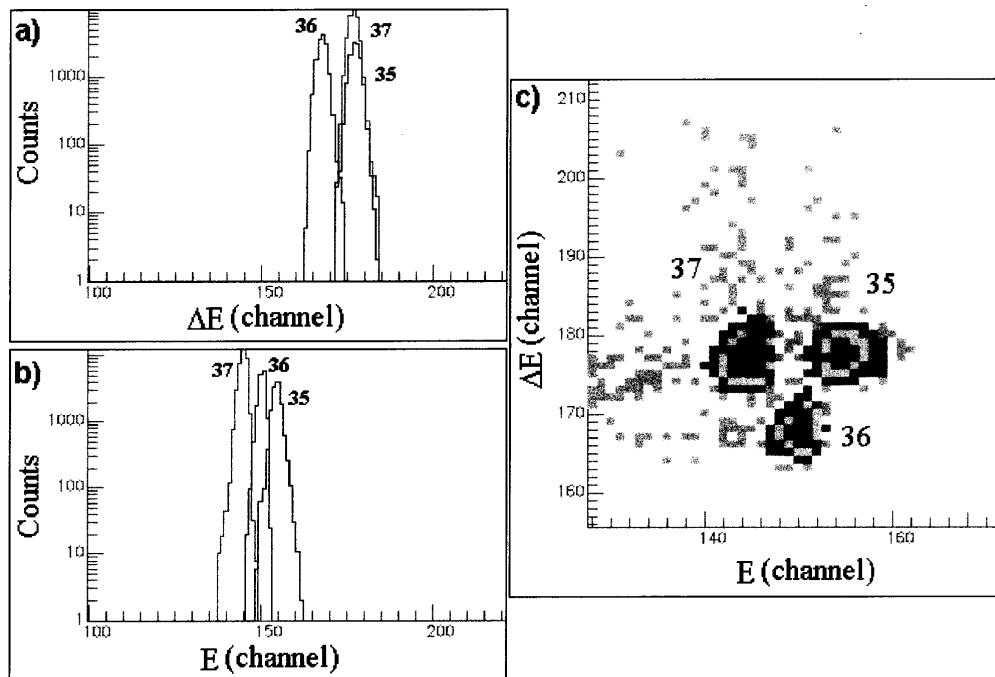


Figure 5. Superposition of spectra of  $^{35}\text{Cl}$ ,  $^{37}\text{Cl}$  and  $^{36}\text{S}$  beams, taken with the detector at zero degree and energies of 64.0 MeV, 60.5 MeV and 62.4 MeV, respectively. (5a)- the projection energy- with energy calibration of 0.34 MeV/channel (5b)- the projection energy loss spectra- with energy calibration of 0.41 MeV/channel (5c)- the biparametric spectra.

## V Conclusions

We have designed and built a Bragg detector. Results obtained in the tests show that it has a very good performance, better than the previously used position sensitive ionization chamber, and comparable with reported Bragg detector performances in the literature [4,5,6]. It is ready to be used for Nuclear Reactions and high precision AMS measurements, since it can separate neighbor charges and isobars. We intend to improve the gas pressure control unit and to test the optimum thickness of the window. Finally, tests with different beam energies will be performed, in order to study the dependence of the resolution with the range of the particles.

## References

- 1 Proceedings of the Intern. Conf. on AMS; Nucl. Instr. Meth. in Phys. Res. **B 52** (1990); **B 92** (1994); **B 123** (1997).
- 2 C. Tenreiro, R.M. Anjos, J.C. Acquadro, G. Kremer, G. Ramirez; Nucl. Instr. Meth. in Phys. Res. **B 92**, 89 (1994).
- 3 G.M. Santos, J.C. Acquadro, R. M. Anjos, P.R.S. Gomes; C. Tenreiro, R. Liguori Neto, M. M. Coimbra, C.R. Apolloni, A.M.M. Maciel, N.H. Medina, M.A. Rizzuto, N. Carlin Filho; Nucl. Instr. Meth. in Phys. Res. **B 123**, 34 (1997).
- 4 C.R. Gruhn, M. Binimi, R. Legrain, R. Loveman, W. Pang, M. Roach, D.K. Scott, A. Shotter, T.J. Symons, J. Wouters, M. Zisman, R. Devries, Y.C. Peng, W. Sondheim; Nucl. Instr. Meth. **196**, 33 (1982).
- 5 C. Schessl, W. Wagner, K. Hartel, P. Kienle, H.J. Koenner, W. Mayer, K.E. Rehm; Nucl. Instr. Meth. **192**, 291 (1982).
- 6 M.F. Vineyard, B.D. Wilkins, D.J. Henderson, D. G. Kovar, C. Beck, C.N. Davids, J.J. Kolata; Nucl. Instr. Meth. in Phys. Res. **A 255**, 507 (1987).
- 7 H.R. Andrews, G.C. Ball, R.M. Brown, R.J.J. Cornett, W.G. Davies, B.F. Greiner, Y. Irahori, V.T. Koslowsky, J. McKay, G.M. Milton, J.C.D. Milton, K.W. Allen; Nucl. Instr. Meth. in Phys. Res. **B 52**, 243 (1990).
- 8 J.F. Ziegler, J.P. Biersack and U. Littmark; *The Stopping and Range of Ions in Solids* Pergamon Press, New York (1985).